Figure 4. C/EBPβ-deficient BMMSCs have an impaired osteogenic differentiation capability. (A, B) Alizarin Red S staining of WT and C/EBPβ-deficient (KO) BMMSCs cultured in osteogenesis-inducing conditions *in vitro*. (A) Representative images. Yellow arrows indicate calcium deposits. Original magnification, 100×. Bars, 50 μm. (B) Calcium deposits were measured in ten different fields at 100× magnification. (C) Immunoblot analysis of Runx2 and ALP expression in WT and C/EBPβ-deficient (KO) BMMSCs cultured in osteogenesis-inducing conditions *in vitro*. Expression levels were measured using densitometry and normalized against the expression level of β-actin. (D) Quantitative real-time PCR analysis examining the expression of ALP mRNA in BMMSCs cultured in osteogenesis-inducing conditions *in vitro*. WT: WT BMMSCs (n = 3), KO: C/EBPβ-deficient BMMSCs (n = 5). (E, F) *In vivo* bone-forming capability of BMMSCs. WT or C/EBPβ-deficient BMMSCs mixed with HA/TCP were subcutaneously implanted into SCID mice. (E) Representative macroscopic appearance of BMMSC implants (left panels). Yellow arrows indicate osseous nodules. Representative microscopic images of sections of BMMSC implants stained with HE (right panels). Original magnification, 40×. Bars, 50 μm. Yellow asterisks indicate bone-forming areas. (F) Bone formation in WT BMMSC implants (WT, n = 6) and C/EBPβ-deficient BMMSC implants (KO, n = 4), as assessed by HE staining. Bone-forming areas at 40× magnification were quantified using Image J software. **, $P < 0.01$.

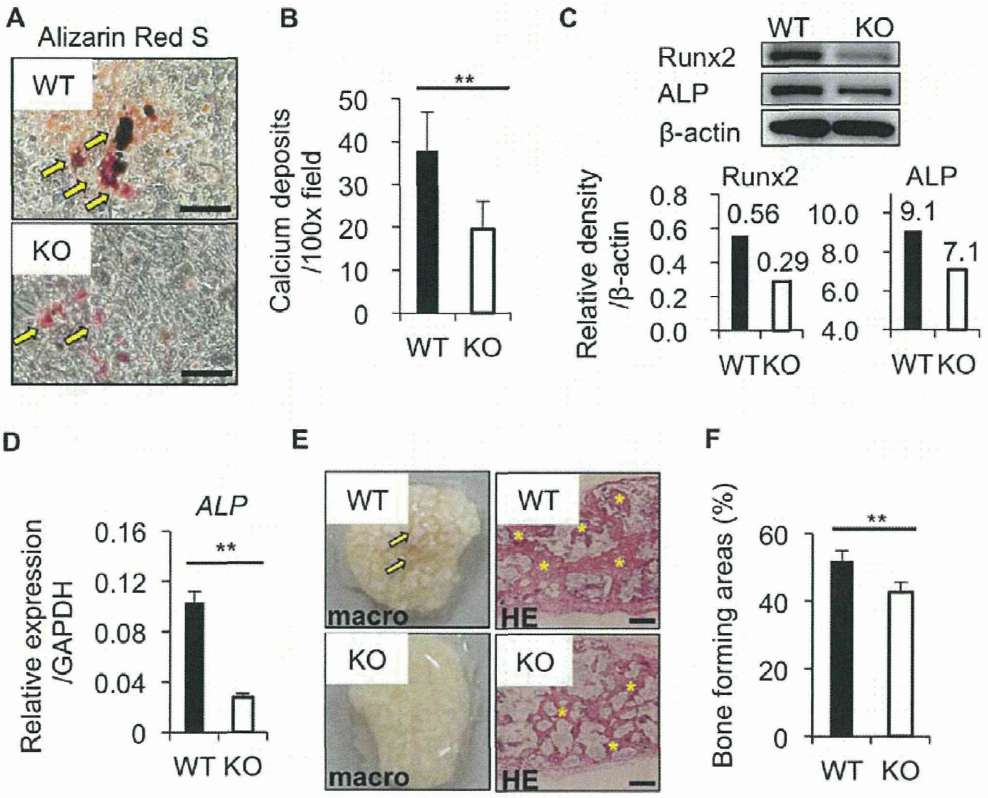

Figure 5. C/EBPβ-deficient BMMSCs have an impaired adipogenic differentiation capability. (A-C) Culture of WT and C/EBPβ-deficient (KO) BMMSCs in adipogenesis-inducing conditions *in vitro*. (A) Representative phase contrast images. Yellow arrows indicate lipid deposition. Original magnification, 100×. Bars, 50 μm. (B, C) Oil Red O staining of WT and C/EBPβ-deficient (KO) BMMSCs cultured in adipogenesis-inducing conditions. (B) Representative images. Yellow arrows indicate lipid deposits. Original magnification, 100×. Bars, 50 μm. (C) The number of Oil Red O^+ cells was measured in ten different fields at 100× magnification. (D) Immunoblot analysis examining the expression of PPARγ, Lpl, and FABP4 in WT and C/EBPβ-deficient (KO) BMMSCs cultured in adipogenesis-inducing conditions *in vitro*. Expression levels were determined using densitometry and normalized against the expression level of β-actin. (E) Quantitative real-time PCR analysis examining the expression of PPARγ, Lpl, and Fabp4 mRNA in BMMSCs cultured in adipogenesis-inducing conditions. WT: WT BMMSCs (n = 5), KO: C/EBPβ-deficient BMMSCs (n = 5). *, $P < 0.05$; **, $P < 0.01$.

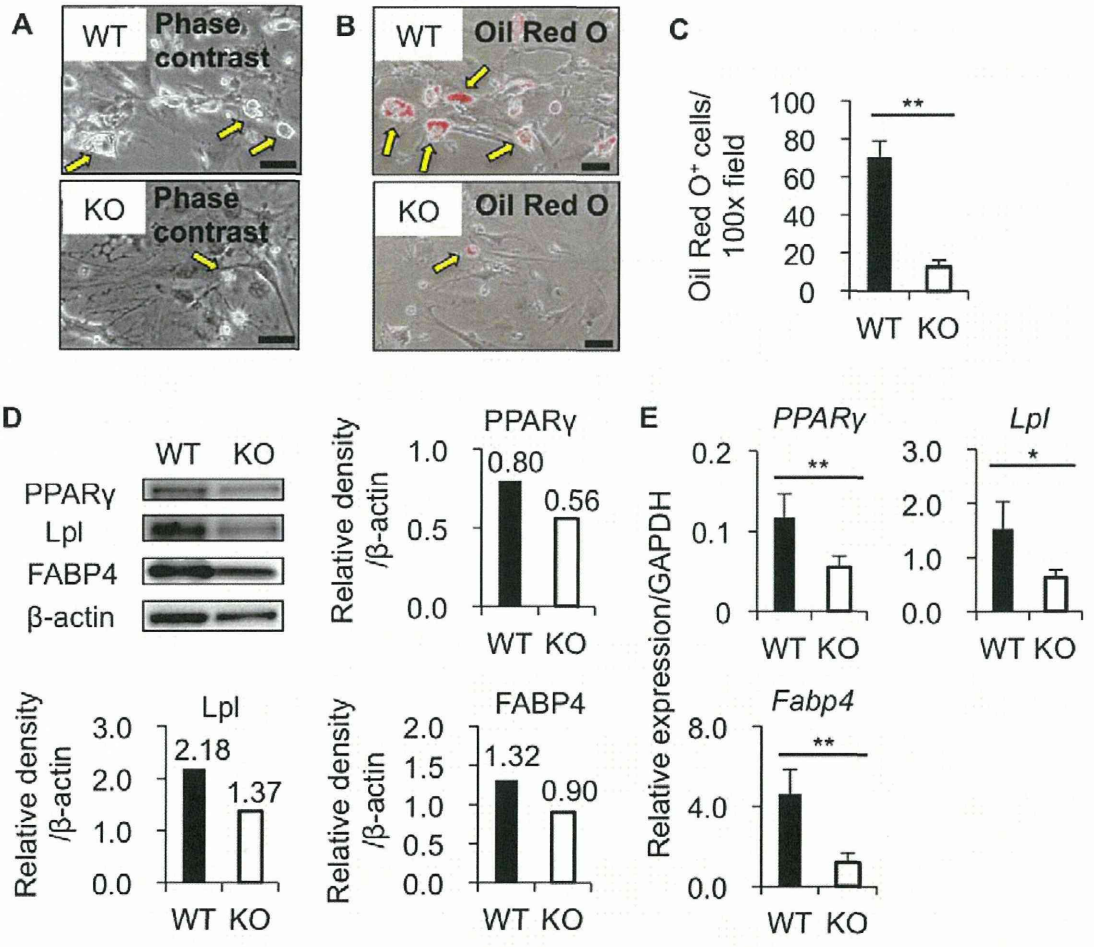

Figure 6. Survival of leukemic precursor B-cells is suppressed when co-cultured with C/EBPβ-deficient BMMSCs. (A) BaF3/Bcr-Abl cells were co-cultured with WT or C/EBPβ-deficient (KO) BMMSCs. (B) Number of BaF3/Bcr-Abl cells when co-cultured with WT (WT, n = 5) or C/EBPβ-deficient (KO) (n = 5) BMMSCs. (C, D) Cell cycle analyses of BaF3/Bcr-Abl cells after co-culture with WT (n = 5) or C/EBPβ-deficient (KO) (n = 5) BMMSCs for 2 days. (C) Representative histograms. (D) The frequencies of BaF3/Bcr-Abl cells at G0/G1, S and G2M phases. Data are mean values ± SD. (F, G) Frequency of apoptotic BaF3/Bcr-Abl cells after co-culture with WT (n = 5) or C/EBPβ-deficient (KO) (n = 5) BMMSCs for 3days. (E) Representative counter plots. Numbers in each box indicate the percentage of cells. (F) Frequencies of Annexin V^-PI^-, Annexin V^+PI^-, and Annexin V^+PI^+ cells. Data are mean absorbance values ± SD. (G) The number of BaF3/Bcr-Abl cells stimulated with exogenous CXCL12/SDF-1 was examined by determing BrdU incorporation using a colorimetric immunoassay (n = 6). Data are mean absorbance values ± SD. *, $P < 0.05$; **, $P < 0.01$.

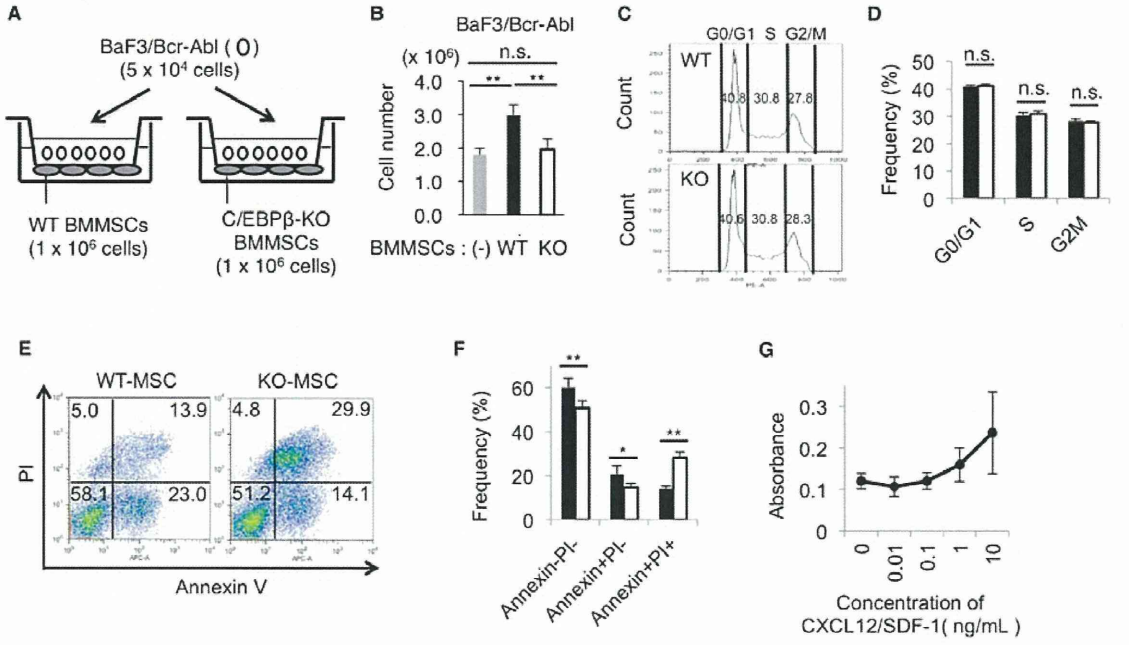

Biochemical and Biophysical Research Communications xxx (2013) xxx–xxx

Contents lists available at ScienceDirect

Biochemical and Biophysical Research Communications

journal homepage: www.elsevier.com/locate/ybbrc

Uric acid induces NADPH oxidase-independent neutrophil extracellular trap formation

Yasuyuki Arai [a,1], Yoko Nishinaka [b,c,1], Toshiyuki Arai [a,d], Makiko Morita [b], Kiyomi Mizugishi [a], Souichi Adachi [b], Akifumi Takaori-Kondo [a], Tomohiro Watanabe [e], Kouhei Yamashita [a,*]

[a] Department of Hematology and Oncology, Graduate School of Medicine, Kyoto University, Kyoto 606-8507, Japan
[b] Human Health Science, Graduate School of Medicine, Kyoto University, Kyoto 606-8507, Japan
[c] Department of Clinical Application, Center for iPS Cell Research and Application, Kyoto University, Kyoto 606-8507, Japan
[d] Department of Anesthesia, Kyoto City Hospital, Kyoto 604-8845, Japan
[e] Center for Innovation in Immunoregulative Technology and Therapeutics, Graduate School of Medicine, Kyoto University, Kyoto 606-8507, Japan

ARTICLE INFO

Article history:
Received 15 November 2013
Available online xxxx

Keywords:
Uric acid
Neutrophil extracellular trap formation
NADPH oxidase
Chronic granulomatous disease
NF-κB
Reactive oxygen species

ABSTRACT

Neutrophil extracellular traps (NETs) are composed of extracellular DNA fibers with antimicrobial peptides that capture and kill microbes. NETs play a critical role in innate host defense and in autoimmune and inflammatory diseases. While the mechanism of NET formation remains unclear, reactive oxygen species (ROS) produced via activation of NADPH oxidase (Nox) are known to be an important requirement. In this study, we investigated the effect of uric acid (UA) on NET formation. UA, a well-known ROS scavenger, was found to suppress Nox-dependent ROS release in a dose-dependent manner. Low concentrations of UA significantly inhibited Nox-dependent NET formation. However, high concentrations of UA unexpectedly induced, rather than inhibited, NET formation. NETs were directly induced by UA alone in a Nox-independent manner, as revealed by experiments using control neutrophils treated with ROS inhibitors or neutrophils of patients with chronic granulomatous disease who have a congenital defect in ROS production. Furthermore, we found that UA-induced NET formation was partially mediated by NF-κB activation. Our study is the first to demonstrate the novel function of UA in NET formation and may provide insight into the management of patients with hyperuricemia.

1. Introduction

Neutrophils, the first line of defense against the microbes, play a critical role in innate immunity [1]. In infected sites, they phagocytose microbes, degranulate enzymes, and produce reactive oxygen species (ROS) such as superoxide and hydrogen peroxide generated by the NADPH oxidase (Nox) complex. Recently, a novel killing mechanism known as neutrophil extracellular traps (NETs) has been reported. NETs capture microbes with their extracellular structures consisting of DNA fibers and antimicrobial granule proteins [2,3]. Many physiological stimuli are known to induce NETs. Notably, NET formation is generally ROS-dependent. Patients with chronic granulomatous disease (CGD), who are defective in Nox activity, fail to generate ROS and to make NETs [4]. In a recent study, we demonstrated that singlet oxygen ($^1O_2$), one species of ROS, is required for Nox-dependent NET formation on stimulation with phorbol myristate acetate (PMA) [5]. Interestingly, neutrophils of CGD patients treated with $^1O_2$ *in vitro* produced NETs, revealing that the pathway could be rescued downstream of Nox [5].

Uric acid (UA), a product of purine metabolism, is a scavenger of $^1O_2$ that regulates oxidative stress in humans [6]. Since $^1O_2$ is produced by Nox [7], UA is expected to suppress Nox-dependent NET formation. However, a recent study showed that peripheral and synovial fluid neutrophils derived from patients with acute gout, whose UA levels in serum were mostly high, formed NETs [8]. Acute gout is an inflammatory arthritis that is triggered by the deposition of monosodium urate (MSU) crystals, uric acid precipitates in sodium, into the joint space. The inflammatory cascade results in the secretion of inflammatory cytokines, especially interleukin (IL)-1ß and neutrophil recruitment into the joint [9]. Thus, it is still a matter of debate what effect UA directly exerts on NET formation.

In the present study, we first examined the effect of UA on Nox-dependent NET formation by control neutrophils stimulated with PMA. Thereafter, we investigated how UA directly affected NET for-

Abbreviations: CGD, chronic granulomatous disease; DHR, dihydrorhodamine 123; DPI, diphenyleneiodonium; HBSS, Hanks' balanced salt solution; MSU, monosodium urate; MVP, trans-1-(2′-methoxyvinyl)pyrene; Nox, NADPH oxidase; NET, neutrophil extracellular trap; PBN, α-phenyl-*N*-tert-butyl nitrone; PMA, phorbol myristate acetate; ROS, reactive oxygen species; $^1O_2$, singlet oxygen; UA, uric acid.

* Corresponding author. Fax: +81 75 751 4963.
E-mail address: kouhei@kuhp.kyoto-u.ac.jp (K. Yamashita).

[1] These authors contributed equally to this work.

0006-291X/$ - see front matter © 2013 Elsevier Inc. All rights reserved.
http://dx.doi.org/10.1016/j.bbrc.2013.12.007

mation by using control neutrophils treated with ROS inhibitors or CGD neutrophils. Finally, we demonstrate that UA may induce NET formation in a manner distinct from that of PMA.

2. Materials and methods

2.1. Reagents

Hanks' balanced salt solution (HBSS) was purchased from Invitrogen (Carlsbad, CA, USA); trans-1-(2′-methoxyvinyl)pyrene (MVP), Sytox green and orange (for double-strand DNA staining), and dihydrorhodamine 123 (DHR) were ordered from Molecular Probes (Eugene, OR, USA). α-Phenyl-*N*-tert-butyl nitrone (PBN) was acquired from Radical Research Ltd. (Hino, Tokyo, Japan) and was dissolved in phosphate-buffered saline (PBS) at a final concentration of 100 mM (pH 7.4). Anti-myeloperoxidase (MPO) antibody and matched secondary antibody (anti-rabbit IgG-Alexa Fluor 488) were obtained from Abcam (Eugene, OR, USA) and Life Technologies (Carlsbad, CA, USA), respectively. Other chemicals, including UA, PMA, diphenyleneiodonium (DPI), and apocynin, were purchased from Sigma Aldrich Inc. (St. Louis, MO, USA). (*E*)3-[(4-Methylphenyl)sulfonyl]-2-propenenitrile (BAY 11-7082) was obtained from Merck (Darmstadt, Germany).

2.2. Human CGD patients

We studied two CGD patients, a 29-year-old man with gp91-phox deficiency with a G-to-A point mutation at nucleotide 252 in exon 3, and a 24-year-old man with gp91-phox deficiency with a G-to-A point mutation at nucleotide 389 in exon 10.

2.3. Isolation of human neutrophils

Human neutrophils were isolated from peripheral blood by sedimentation through two-step Percoll (GE Healthcare, Tokyo, Japan) gradients. The experiments were conducted with the understanding and the consent of each participant. The ethical committee of Kyoto University approved the experiments.

2.4. Chemiluminescence assay

Neutrophils (2×10^6 cells) were mounted on a luminescence reader (Aloka BLR-310; Aloka, Tokyo, Japan) in the presence of 40 μM MVP, a $^1O_2$-specific probe [10]. After that, neutrophils were stimulated with 100 ng/ml PMA in the presence of 0–5 mg/dl UA, or 8 mg/dl UA alone, and MVP luminescence was monitored every 30 s for 30 min.

2.5. Flow cytometric DHR assay

Neutrophils (1×10^6 cells) treated with 2 μM DHR were stimulated with 100 ng/ml PMA or 8 mg/dl UA for 30 min at 37 °C and analyzed by flow cytometry using a FACSCanto II (Becton Dickinson, Durham, NC, USA).

2.6. Immunofluorescence stainings of NET-forming neutrophils

Purified neutrophils (1×10^5 cells) were incubated with 100 ng/ml PMA or 8 mg/dl UA in HBSS without serum for 3 h on culture slides (BD Biosciences, San Jose, CA, USA). After fixation with 2% paraformaldehyde (Nacalai Tesque, Kyoto, Japan) for 15 min and

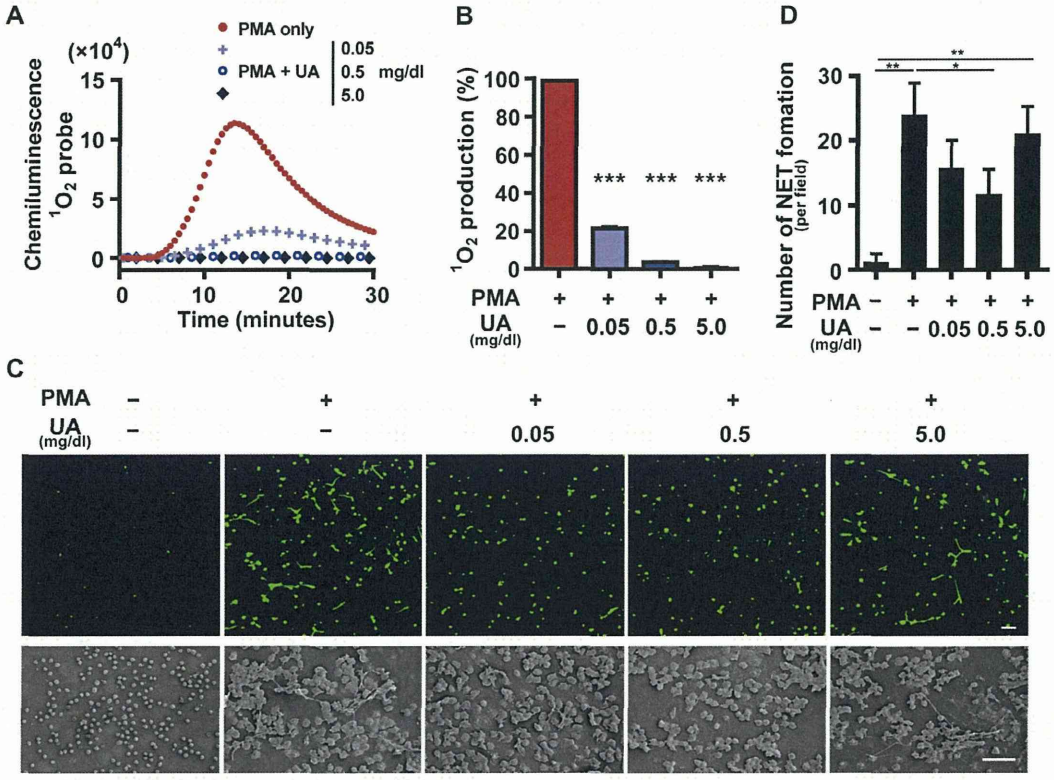

Fig. 1. The effect of UA on PMA-induced ROS production and NET formation. Neutrophils were isolated from the peripheral blood of healthy volunteers. (A) The effect of UA (0–5 mg/dl) on $^1O_2$ production by PMA-stimulated neutrophils. The $^1O_2$ production by neutrophils was examined by chemiluminescence using a $^1O_2$-specific probe, MVP. (B) Quantitative analysis of $^1O_2$ production by neutrophils. The $^1O_2$ production is shown relative to that by PMA-stimulated neutrophils in the absence of UA. The data represent the mean ± SE ($n = 3$, $^{***}P < 0.001$, unpaired *t*-test). (C) The effect of UA on PMA-induced NET formation. Neutrophils stimulated with PMA were incubated with 0–5 mg/dl UA. NET formation was visualized by laser-scanning fluorescence confocal microscopy (upper panels) and SEM (lower panels). Scale bars represent 100 μm (upper panels) and 30 μm (lower panels). (D) Quantitative analysis of NET formation. The data represent the mean ± SE ($n = 4$, $^{*}P < 0.05$, $^{**}P < 0.01$, unpaired *t*-test).

Please cite this article in press as: Y. Arai et al., Uric acid induces NADPH oxidase-independent neutrophil extracellular trap formation, Biochem. Biophys. Res. Commun. (2013), http://dx.doi.org/10.1016/j.bbrc.2013.12.007

permeabilization with 100% methanol (Nacalai Tesque) for 10 min at -20 °C, the cells were stained with rabbit anti-MPO antibodies overnight at 4 °C, followed by Alexa Fluor 488-conjugated goat anti-rabbit IgG and Sytox orange. The cells were attached to the slides by centrifugation, coverslipped with mounting medium (ProLong Gold Antifade Reagent, Life Technologies), and analyzed by confocal microscopy.

2.7. NET formation by neutrophils

Neutrophils (4×10^6 cells) from healthy volunteers were suspended in HBSS without serum and stimulated with 100 ng/ml PMA in the presence of 0–5 mg/dl UA for 3 h at 37 °C under 5% CO_2 in glass base dish (Asahi Glass, Tokyo, Japan). In other experiments, neutrophils from healthy volunteers or CGD patients were stimulated with 1–8 mg/dl UA alone. After incubation, cells were stained with 500 nM Sytox Green, and NET formation was visualized with a laser-scanning fluorescence confocal microscope (Nikon Digital Eclipse C1, Tokyo, Japan). Quantitative analysis was performed by counting the number of NET-forming cells per field (average data of 5 randomly selected fields). NET formation was also visualized with a scanning electron microscope (SEM, S-4700, Hitachi, Tokyo, Japan).

2.8. Treatments of neutrophils with inhibitors

Neutrophils (4×10^6 cells) from healthy volunteers were pre-incubated at 37 °C for 30 min with Nox inhibitors, DPI (10 μM) and apocynin (10 μM), a $^1O_2$ inhibitor, PBN (4 mM) [11], or an NF-κB inhibitor, Bay 11-7082 (10 μM), and then stimulated with 100 ng/ml PMA or 8 mg/dl UA for 3 h. NET formation was visualized and analyzed as described above.

2.9. Immunoblotting

Neutrophils (4×10^6 cells) from healthy volunteers were incubated at 37 °C for 30 min with 100 ng/ml PMA or 8 mg/dl UA. Lysates were prepared using RIPA lysis buffer (Wako Pure Chemical Industries, Osaka, Japan). Cell debris was separated by centrifugation and equal amounts of proteins in the supernatant were separated by electrophoresis (4–12% SDS–polyacrylamide gels, Life Technologies). Proteins were then electrotransferred onto nitrocel-

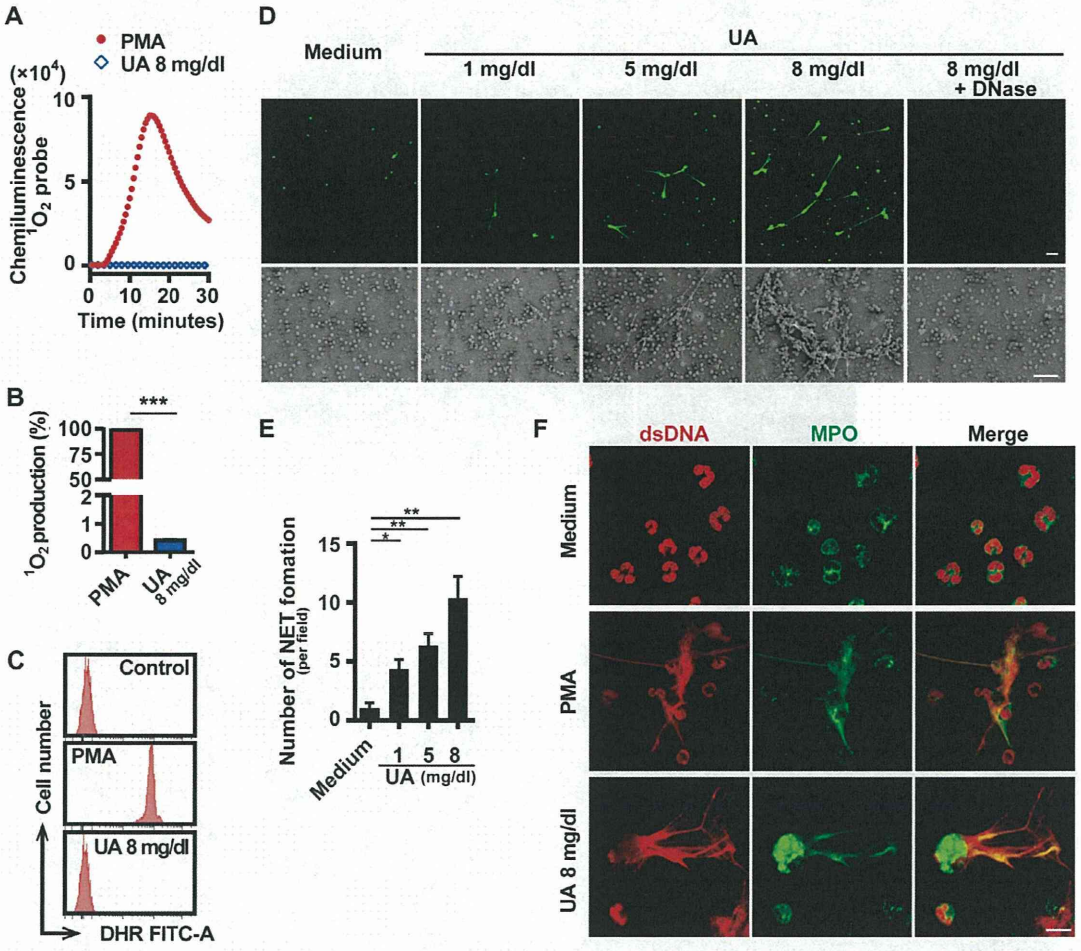

Fig. 2. The effect of UA alone on ROS production and NET formation. (A and B) Effect of UA on $^1O_2$ production. Neutrophils were stimulated with PMA (100 ng/ml) or UA (8 mg/dl). $^1O_2$ production was examined by chemiluminescence using a $^1O_2$-specific probe, MVP. (A) Representative data. UA-stimulated neutrophils hardly produced any $^1O_2$. (B) Quantitative analysis of $^1O_2$ production shown relative to that by PMA-stimulated neutrophils. Data represent mean ± SE ($n = 3$, $^{***}P < 0.001$, unpaired t-test). (C) ROS production by DHR assay. The logarithmic fluorescence intensity is shown on the x-axis and the cell count on the y-axis. (D–F) Direct effect of UA on NET formation. (D) Representative micrographs of neutrophils incubated with 1–8 mg/dl of UA. NET formation was visualized by laser-scanning fluorescence confocal microscopy (upper panels) and SEM (lower panels). Scale bars represent 100 μm (upper panels) and 30 μm (lower panels). (E) Quantitative analysis of NET formation. Data represent the mean ± SE ($n = 5$, $^{*}P < 0.05$, $^{**}P < 0.01$, unpaired t-test). (F) Colocalization of extracellular dsDNA and MPO in UA-stimulated neutrophils. UA- or PMA-stimulated neutrophils were immunostained with anti-MPO antibody (green). The dsDNAs were counterstained with Sytox-orange (red). Scale bars represent 10 μm. (For interpretation of the references to color in this figure legend, the reader is referred to the web version of this article.)

Please cite this article in press as: Y. Arai et al., Uric acid induces NADPH oxidase-independent neutrophil extracellular trap formation, Biochem. Biophys. Res. Commun. (2013), http://dx.doi.org/10.1016/j.bbrc.2013.12.007

lulose membranes. After blocking, membranes were incubated overnight at 4 °C with a rabbit polyclonal anti-phospho-NF-κB p65 or anti-NF-κB p65 antibody (Santa Cruz Biotechnology, Dallas, TX, USA) followed by a goat anti-rabbit HRP antibody. Protein bands were visualized by enhanced chemiluminescence, and results were analyzed with ImageJ software.

2.10. Statistical analysis

Data were expressed as mean ± standard error (SE). Values of $P < 0.05$ determined by the unpaired Student t-test were considered significant.

3. Results and discussion

We examined the effect of UA on $^1O_2$ production and NET formation by PMA-stimulated neutrophils. First, neutrophils from healthy volunteers were stimulated with PMA with or without UA, and the $^1O_2$ production was detected by chemiluminescence. As expected, increasing concentrations of UA (0.05–5 mg/dl) suppressed $^1O_2$ production by PMA-stimulated neutrophils in a dose-dependent manner, suggesting that UA is a $^1O_2$ scavenger (Fig. 1A and B). Treatments of less than 0.5 mg/dl of UA suppressed PMA-induced NET formation in confocal microscopy (Fig. 1C, upper panels, and Fig. 1D) and SEM (Fig. 1C, lower panels). Surprisingly, treatment of PMA-stimulated neutrophils with 5 mg/dl of UA failed to suppress NET formation, suggesting that a high concentration of UA may have a novel function in NET formation (Fig. 1C and D). These results were substantiated by the quantitative analysis of representative micrographs (Fig. 1D).

Next, we investigated the direct effect of UA on $^1O_2$ production and NET formation. UA treatment alone did not produce any detectable levels of $^1O_2$ (Fig. 2A and B). We used the fluorescent dye DHR in a flow cytometric assay to detect ROS. UA-stimulated neutrophils from healthy volunteers did not exhibit any increase in DHR fluorescence, in contrast to a significant increase in PMA-stimulated neutrophils (Fig. 2C). Unexpectedly, UA alone

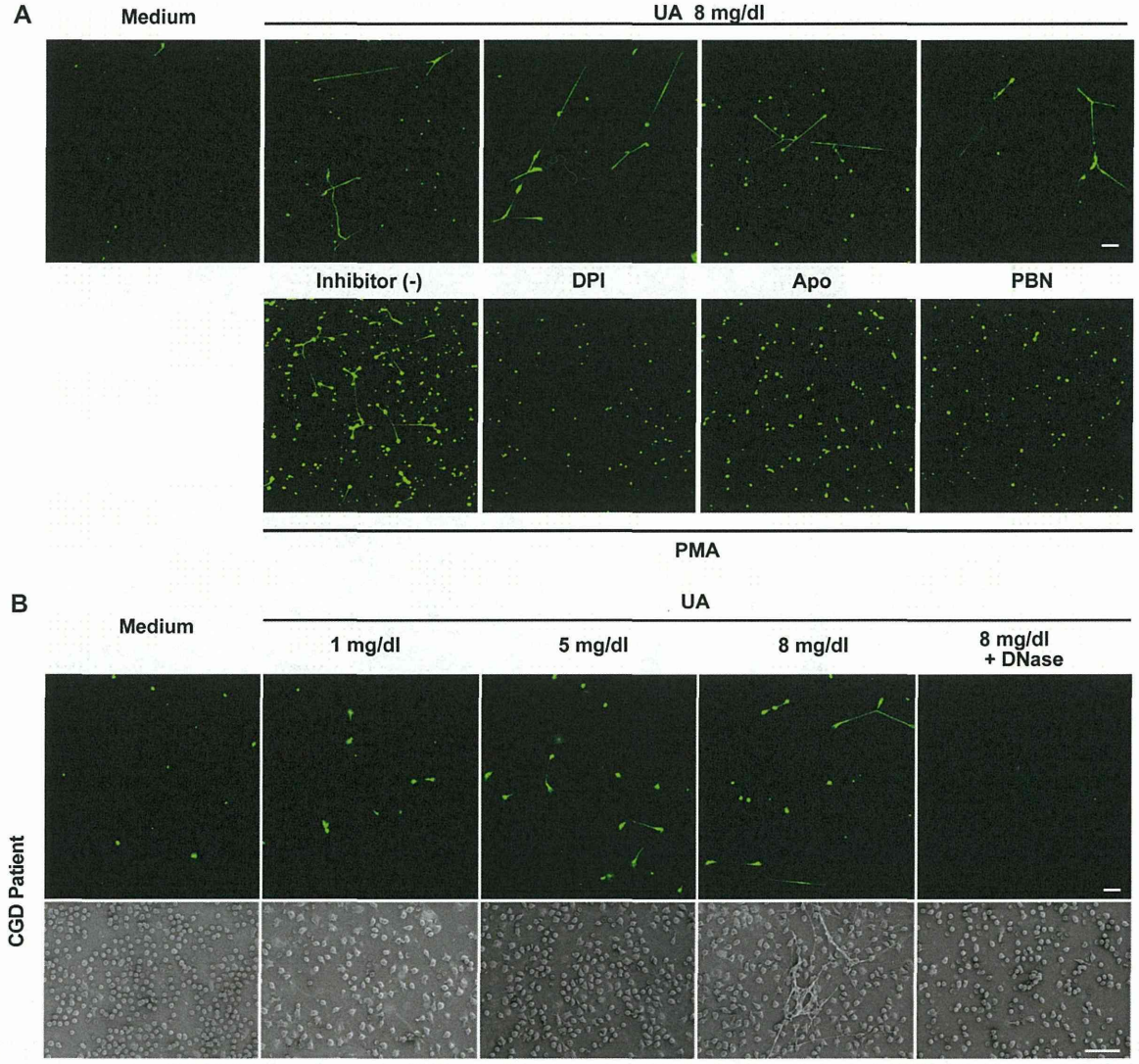

Fig. 3. UA-induced NET formation is independent of ROS. (A) The effect of ROS inhibitors on UA- (upper panels) or PMA- (lower panels) induced NET formation. Neutrophils from healthy volunteers were incubated with 8 mg/dl UA or 100 ng/ml PMA in the presence or absence of Nox inhibitors, DPI and apocynin (Apo), or a $^1O_2$ inhibitor, PBN. NET formation was visualized by laser-scanning fluorescence confocal microscopy. Scale bars represent 100 μm. (B) The effect of UA on NET formation. Neutrophils from CGD patients were incubated with 1–8 mg/dl of UA. Representative micrographs are shown. NET formation was visualized by laser-scanning fluorescence confocal microscopy (upper panels) and SEM (lower panels). Scale bars represent 100 μm (upper panels) and 30 μm (lower panels).

Please cite this article in press as: Y. Arai et al., Uric acid induces NADPH oxidase-independent neutrophil extracellular trap formation, Biochem. Biophys. Res. Commun. (2013), http://dx.doi.org/10.1016/j.bbrc.2013.12.007

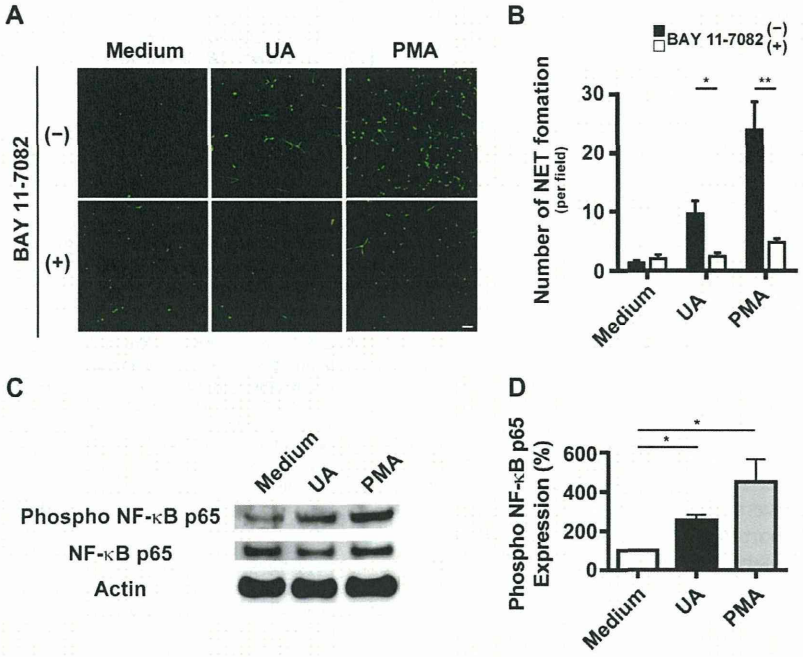

Fig. 4. UA induces NET formation through NF-κB activation. (A and B) The effect of an NF-κB inhibitor on UA-induced NET formation. Neutrophils from healthy volunteers were stimulated with 100 ng/ml PMA or 8 mg/dl UA in the presence or absence of an NF-κB inhibitor. (A) Representative micrographs. NET formation was visualized by laser-scanning fluorescence confocal microscopy. Scale bars represent 100 μm. (B) Quantitative analysis of NET formation. The data represent the mean ± SE ($n = 5$, $^*P < 0.05$, $^{**}P < 0.01$, unpaired t-test). (C) Immunoblot analysis of PMA- or UA-stimulated neutrophils. Cell lysates were subjected to immunoblotting using an anti-phospho-NF-κB p65 or anti-NF-κB p65 antibody. Membranes were reprobed with an anti-actin antibody. (D) Quantification of proteins on immunoblots. The expression levels are shown relative to that in neutrophils without stimuli. The data represent the mean ± SE ($n = 5$, $^*P < 0.05$, unpaired t-test).

significantly induced NET formation in healthy neutrophils, irrespective of the absence of ROS (Fig. 2D and E). NET formation was abrogated by DNase treatment, which degrades DNA fibers of NETs (Fig. 2D). NET formation by UA was further verified by immunostaining, in which extracellular dsDNA colocalized with a granule protein MPO, an important structural component of NETs (Fig. 2F). These results suggest that NET formation by UA may not be mediated by ROS.

This hypothesis was substantiated by the use of Nox inhibitors, DPI and apocynin, or a $^1O_2$ scavenger, PBN. None of the ROS inhibitors suppressed UA-induced NET formation, while PMA-induced NETs were strongly inhibited (Fig. 3A). We next examined NET formation in neutrophils from CGD patients, who have a defect in ROS formation. Regardless of the absence of ROS, CGD neutrophils treated with UA produced NETs, which were suppressed by DNase treatment (Fig. 3B). Taken together, these results suggest that UA may induce NET formation in a Nox-independent manner.

Recently, Lopponi et al. implicated NF-κB activation in NET formation induced by PMA stimulus or stress signals, such as acidic or hyperthermic conditions [12]. Therefore, we investigated whether NF-κB blockade affected NET formation by UA-stimulated neutrophils. The treatment of healthy neutrophils with the NF-κB inhibitor BAY 11-7082 resulted in a marked suppression of UA-induced NET formation (Fig. 4A and B). In addition, immunoblot analysis revealed that phosphorylation of the p65 subunit of NF-κB was significantly enhanced in neutrophils stimulated with UA (Fig. 4C and D). Taken together, these results suggest that the NF-κB cascade is important in UA-mediated NET formation, and could be a key regulatory pathway of NET formation. Identification of signaling pathways upstream of NF-κB in UA-induced NET formation should be a future area of investigation.

In summary, this is the first report to demonstrate the novel function of UA in NET formation. Contrary to expectations, UA, a known $^1O_2$ scavenger, induced NETs in neutrophils in a Nox-independent manner and partially through activation of the NF-κB pathway. The mechanisms by which UA contributes to NET formation are not yet clear. It has been reported that the Raf-MEK-ERK pathway is involved in a NET formation cascade downstream of Nox activation in PMA-stimulated neutrophils [13]. Furthermore, MSU crystals induced NETs in a ROS-dependent manner as well as PMA [14]. In contrast, NET formation by UA was independent of ROS. In addition, neither the activation of ERK, nor the suppression of NETs by an ERK inhibitor, was observed in UA-stimulated neutrophils in our study (unpublished observation). This suggests that UA induces NETs in a different fashion from that of PMA and MSU crystals. An example of ROS-independent NET formation was reported in a recent study, where the calcium ionophore ionomycin did not require Nox activation to induce NETs [15]. Moreover, *Staphylococcus aureus* and *Candida albicans* have been reported to induce NETs independently of Nox [16,17]. Thus, it is possible that there are several mechanisms of NET formation. The importance of a ROS-independent pathway in NET formation in physiological settings awaits further investigation.

NETs are similar to a double-edged sword; they can either fight disease or cause disease, depending on the situation [18]. Excessive NET formation is associated with the pathogenesis of inflammatory and autoimmune diseases, including preeclampsia [19], cystic fibrosis [20], and systemic lupus erythematosus [21]. Moreover, NETs are relevant to vascular injury, in which extracellular histones released from neutrophils during NET formation injure the endothelium [22], and the injured endothelium, in turn, induces NETs, establishing a vicious cycle leading to severe damage [23]. Clinically, the association of hyperuricemia and gout with other medical conditions such as hypertension, chronic kidney disease, and cardiovascular disease has been recognized [24]. Recent animal and epidemiologic studies support the idea that uric acid elevation in the serum is an independent risk factor for the development of these serious medical problems, by damaging

Please cite this article in press as: Y. Arai et al., Uric acid induces NADPH oxidase-independent neutrophil extracellular trap formation, Biochem. Biophys. Res. Commun. (2013), http://dx.doi.org/10.1016/j.bbrc.2013.12.007

endothelial cells, although it is still a matter of debate [25]. In light of these findings, we speculate that uric acid elevation may induce NET formation and subsequent vascular endothelial dysfunction, ultimately leading to cardiovascular diseases. Therefore, NETs could be a missing link between uric acid elevation and cardiovascular diseases. Thus, we may need to reappraise the importance of uric acid in human health and disease, and reconsider the management of patients with asymptomatic hyperuricemia in order to decrease the risk of cardiovascular diseases.

Conflict of interest disclosure

The authors declare no conflict of interest.

Acknowledgments

We thank Keiko Furuta and Haruyasu Kohda (Division of Electron Microscopic Study, Center for Anatomical Studies, Graduate School of Medicine, Kyoto University) for excellent technical assistance. This research was supported by Grants-in-aid for scientific research from the Japan Society for the Promotion of Science (23591474) to K.Y.

References

[1] C. Nathan, Neutrophils and immunity: challenges and opportunities, Nat. Rev. Immunol. 6 (2006) 173–182.
[2] V. Brinkmann, U. Reichard, C. Goosmann, B. Fauler, Y. Uhlemann, D.S. Weiss, Y. Weinrauch, A. Zychlinsky, Neutrophil extracellular traps kill bacteria, Science 303 (2004) 1532–1535.
[3] V. Brinkmann, A. Zychlinsky, Beneficial suicide: why neutrophils die to make NETs, Nat. Rev. Microbiol. 5 (2007) 577–582.
[4] T.A. Fuchs, U. Abed, C. Goosmann, R. Hurwitz, I. Schulze, V. Wahn, Y. Weinrauch, V. Brinkmann, A. Zychlinsky, Novel cell death program leads to neutrophil extracellular traps, J. Cell Biol. 176 (2007) 231–241.
[5] Y. Nishinaka, T. Arai, S. Adachi, A. Takaori-Kondo, K. Yamashita, Singlet oxygen is essential for neutrophil extracellular trap formation, Biochem. Biophys. Res. Commun. 413 (2011) 75–79.
[6] B.N. Ames, R. Cathcart, E. Schwiers, P. Hochstein, Uric acid provides an antioxidant defense in humans against oxidant- and radical-caused aging and cancer: a hypothesis, Proc. Natl. Acad. Sci. U.S.A. 78 (1981) 6858–6862.
[7] S.J. Klebanoff, Myeloperoxidase: friend and foe, J. Leukocyte Biol. 77 (2005) 598–625.
[8] I. Mitroulis, K. Kambas, A. Chrysanthopoulou, P. Skendros, E. Apostolidou, I. Kourtzelis, G.I. Drosos, D.T. Boumpas, K. Ritis, Neutrophil extracellular trap formation is associated with IL-1beta and autophagy-related signaling in gout, PLoS One 6 (2011) e29318.
[9] E.B. Gonzalez, An update on the pathology and clinical management of gouty arthritis, Clin. Rheumatol. 31 (2012) 13–21.
[10] G.H. Posner, J.R. Lever, K. Miura, C. Lisek, H.H. Seliger, A. Thompson, A chemiluminescent probe specific for singlet oxygen, Biochem. Biophys. Res. Commun. 123 (1984) 869–873.
[11] A. Kawai, Y. Nishinaka, T. Arai, K. Hirota, H. Mori, N. Endo, T. Miyoshi, K. Yamashita, M. Sasada, Alpha-phenyl-*N*-tert-butyl nitrone has scavenging activity against singlet oxygen ((1)O(2)) and attenuates (1)O(2)-induced neuronal cell death, J. Pharmacol. Sci. 108 (2008) 545–549.
[12] M.J. Lapponi, A. Carestia, V.I. Landoni, L. Rivadeneyra, J. Etulain, S. Negrotto, R.G. Pozner, M. Schattner, Regulation of neutrophil extracellular trap formation by anti-inflammatory drugs, J. Pharmacol. Exp. Ther. 345 (2013) 430–437.
[13] A. Hakkim, T.A. Fuchs, N.E. Martinez, S. Hess, H. Prinz, A. Zychlinsky, H. Waldmann, Activation of the Raf-MEK-ERK pathway is required for neutrophil extracellular trap formation, Nat. Chem. Biol. 7 (2011) 75–77.
[14] C. Schorn, C. Janko, V. Krenn, Y. Zhao, L.E. Munoz, G. Schett, M. Herrmann, Bonding the foe – NETting neutrophils immobilize the pro-inflammatory monosodium urate crystals, Front. Immunol. 3 (2012) 376.
[15] H. Parker, M. Dragunow, M.B. Hampton, A.J. Kettle, C.C. Winterbourn, Requirements for NADPH oxidase and myeloperoxidase in neutrophil extracellular trap formation differ depending on the stimulus, J. Leukocyte Biol. 92 (2012) 841–849.
[16] F.H. Pilsczek, D. Salina, K.K. Poon, C. Fahey, B.G. Yipp, C.D. Sibley, S.M. Robbins, F.H. Green, M.G. Surette, M. Sugai, M.G. Bowden, M. Hussain, K. Zhang, P. Kubes, A novel mechanism of rapid nuclear neutrophil extracellular trap formation in response to Staphylococcus aureus, J. Immunol. 185 (2010) 7413–7425.
[17] A.S. Byrd, X.M. O'Brien, C.M. Johnson, L.M. Lavigne, J.S. Reichner, An extracellular matrix-based mechanism of rapid neutrophil extracellular trap formation in response to Candida albicans, J. Immunol. 190 (2013) 4136–4148.
[18] V. Brinkmann, A. Zychlinsky, Neutrophil extracellular traps: is immunity the second function of chromatin?, J Cell Biol. 198 (2012) 773–783.
[19] A.K. Gupta, P. Hasler, W. Holzgreve, S. Gebhardt, S. Hahn, Induction of neutrophil extracellular DNA lattices by placental microparticles and IL-8 and their presence in preeclampsia, Hum. Immunol. 66 (2005) 1146–1154.
[20] R. Manzenreiter, F. Kienberger, V. Marcos, K. Schilcher, W.D. Krautgartner, A. Obermayer, M. Huml, W. Stoiber, A. Hector, M. Griese, M. Hannig, M. Studnicka, L. Vitkov, D. Hartl, Ultrastructural characterization of cystic fibrosis sputum using atomic force and scanning electron microscopy, J. Cyst. Fibros. 11 (2012) 84–92.
[21] A. Hakkim, B.G. Furnrohr, K. Amann, B. Laube, U.A. Abed, V. Brinkmann, M. Herrmann, R.E. Voll, A. Zychlinsky, Impairment of neutrophil extracellular trap degradation is associated with lupus nephritis, Proc. Natl. Acad. Sci. U.S.A. 107 (2010) 9813–9818.
[22] J. Xu, X. Zhang, R. Pelayo, M. Monestier, C.T. Ammollo, F. Semeraro, F.B. Taylor, N.L. Esmon, F. Lupu, C.T. Esmon, Extracellular histones are major mediators of death in sepsis, Nat. Med. 15 (2009) 1318–1321.
[23] A.K. Gupta, M.B. Joshi, M. Philippova, P. Erne, P. Hasler, S. Hahn, T.J. Resink, Activated endothelial cells induce neutrophil extracellular traps and are susceptible to NETosis-mediated cell death, FEBS Lett. 584 (2010) 3193–3197.
[24] D.I. Feig, D.H. Kang, R.J. Johnson, Uric acid and cardiovascular risk, N. Engl. J. Med. 359 (2008) 1811–1821.
[25] N.L. Edwards, The role of hyperuricemia in vascular disorders, Curr. Opin. Rheumatol. 21 (2009) 132–137.

Please cite this article in press as: Y. Arai et al., Uric acid induces NADPH oxidase-independent neutrophil extracellular trap formation, Biochem. Biophys. Res. Commun. (2013), http://dx.doi.org/10.1016/j.bbrc.2013.12.007

OPEN ACCESS Freely available online

PLOS ONE

CKIP-1 Is an Intrinsic Negative Regulator of T-Cell Activation through an Interaction with CARMA1

Takashi Sakamoto[1], Masayuki Kobayashi[1]*, Kohei Tada[1], Masanobu Shinohara[1], Katsuhiro Io[1], Kayoko Nagata[1], Fumie Iwai[1], Yoko Takiuchi[1], Yasuyuki Arai[1], Kouhei Yamashita[1], Keisuke Shindo[1], Norimitsu Kadowaki[1], Yoshio Koyanagi[2], Akifumi Takaori-Kondo[1]

1 Department of Hematology and Oncology, Graduate School of Medicine, Kyoto University, Kyoto, Japan, **2** Laboratory of Viral Pathogenesis, Institute for Virus Research, Kyoto University, Kyoto, Japan

Abstract

The transcription factor NF-κB plays a key regulatory role in lymphocyte activation and generation of immune response. Stimulation of T cell receptor (TCR) induces phosphorylation of CARMA1 by PKCθ, resulting in formation of CARMA1-Bcl10-MALT1 (CBM) complex at lipid rafts and subsequently leading to NF-κB activation. While many molecular events leading to NF-κB activation have been reported, it is less understood how this activation is negatively regulated. We performed a cell-based screening for negative regulators of TCR-mediated NF-κB activation, using mutagenesis and complementation cloning strategies. Here we show that casein kinase-2 interacting protein-1 (CKIP-1) suppresses PKCθ-CBM-NF-κB signaling. We found that CKIP-1 interacts with CARMA1 and competes with PKCθ for association. We further confirmed that a PH domain of CKIP-1 is required for association with CARMA1 and its inhibitory effect. CKIP-1 represses NF-κB activity in unstimulated cells, and inhibits NF-κB activation induced by stimulation with PMA or constitutively active PKCθ, but not by stimulation with TNFα. Interestingly, CKIP-1 does not inhibit NF-κB activation induced by CD3/CD28 costimulation, which caused dissociation of CKIP-1 from lipid rafts. These data suggest that CKIP-1 contributes maintenance of a resting state on NF-κB activity or prevents T cells from being activated by inadequate signaling. In conclusion, we demonstrate that CKIP-1 interacts with CARMA1 and has an inhibitory effect on PKCθ-CBM-NF-κB signaling.

Citation: Sakamoto T, Kobayashi M, Tada K, Shinohara M, Io K, et al. (2014) CKIP-1 Is an Intrinsic Negative Regulator of T-Cell Activation through an Interaction with CARMA1. PLoS ONE 9(1): e85762. doi:10.1371/journal.pone.0085762

Editor: Kjetil Tasken, University of Oslo, Norway

Received September 16, 2013; **Accepted** December 5, 2013; **Published** January 17, 2014

Funding: This work was supported by JSPS KAKENHI Grant Number 23591383. The URL is http://www.jsps.go.jp/j-grantsinaid/. The funders had no role in study design, data collection and analysis, decision to publish, or preparation of the manuscript.

Competing Interests: The authors have declared that no competing interests exist.

* E-mail: mkobayas@kuhp.kyoto-u.ac.jp

Introduction

The NF-κB family of transcription factors plays a key regulatory role in lymphocyte activation and generation of immune response [1]. The respective NF-κB target genes allow the organism to respond effectively to the environmental changes. Engagement of TCR by specific antigen presented on major histocompatibility complex (MHC) of antigen presenting cells (APC) induces T cell activation and proliferation. However, stimulation of TCR/CD3 complex alone is not sufficient for activation of NF-κB. The simultaneous costimulation of CD28 through its ligand, B7, is needed for optimal activation of NF-κB [2]. CD3/CD28 costimulation induces the formation of a large multicomponent complex at the contact site between T cell and the APC, termed as immunological synapse [3,4]. This contact area of T cells is highly enriched in cholesterol and glycosphingo-lipids, also termed as lipid rafts, and serve as the platform for the assembly of proximal signaling components of TCR. PKCθ is recruited to the immunological synapse from the cytosol upon T cell stimulation and catalytically activated [5,6]. Activated PKCθ phosphorylates CARMA1 (CARD11) to induce its conformational changes which enable CARMA1 to form the complex with Bcl10-MALT1 [7,8]. Subsequently, the IκB kinase (IKK) complex becomes activated and phosphorylates IκBs, leading to their ubiquitylation and subsequent proteasomal degradation. The degradation of IκBs allows NF-κB to enter the nucleus and induce transcription of target genes [1].

CARMA1 is one of a family of caspase recruitment domain (CARD)- and membrane associated guanylate kinase-like (MAGUK) domain-containing proteins (CARMA) [9,10]. CARMA1 contains an N-terminal CARD, followed by a coiled-coil (CC) domain, a PDZ domain, a Src homology 3 (SH3) domain, and a guanylate kinase (GUK)-like domain in the C-terminus. It has two mammalian homologs, CARMA2 and CARMA3. CARMA1 is predominantly expressed in spleen, thymus, and peripheral blood leukocyte (PBL); CARMA2 is expressed only in placenta; and CARMA3 is expressed in broad range of tissues but not in spleen, thymus or PBL. For B and T cells, the scaffold protein CARMA1 plays an essential role in antigen receptor-induced NF-κB activation [11–15]. Aberrant NF-κB activation could be involved in autoimmune diseases and malignant lymphomas. Constitutively active NF-κB in the activated B cell-like (ABC) subtype of diffuse large B cell lymphoma (DLBCL) can result from somatic mutations in genes involved in NF-κB signaling, such as CD79B, A20 and CARMA1 [16]. Recently, germline mutations in CARMA1 have also been reported in four patients with congenital B cell lymphocytosis [17]. Therefore CARMA1 activity needs to be tightly regulated.